

Hybrid CV-DV Quantum Communications and Quantum Networks

IVAN B. DJORDJEVIC¹, (Fellow, IEEE)

Department of Electrical and Computer Engineering, The University of Arizona, Tucson, AZ 85721, USA

e-mail: ivan@email.arizona.edu

This work was supported in part by NSF.

ABSTRACT Quantum information processing (QIP) opens new opportunities for high-performance computing, high-precision sensing, and secure communications. Among various QIP features, the entanglement is a unique one. To take full advantage of quantum resources, it will be necessary to interface quantum systems based on different encodings of information both discrete and continuous. The goal of this paper is to lay the groundwork for the development of a robust and efficient hybrid continuous variable-discrete variable (CV-DV) quantum network, enabling the distribution of a large number of entangled states over hybrid DV-CV multi-hop nodes in an arbitrary topology. The proposed hybrid quantum communication network (QCN) can serve as the backbone for a future quantum Internet, thus providing extensive long-term impacts on the economy and national security through QIP, distributed quantum computing, quantum networking, and distributed quantum sensing. By employing the photon addition and photon subtraction modules we describe how to generate the hybrid DV-CV entangled states and how to implement their teleportation and entanglement swapping through entangling measurements. We then describe how to extend the transmission distance between nodes in hybrid QCN by employing macroscopic light states, noiseless amplification, and reconfigurable quantum LDPC coding. We further describe how to enable quantum networking and distributed quantum computing by employing the deterministic cluster state concept introduced here. Finally, we describe how the proposed hybrid CV-DV states can be used in an entanglement-based hybrid QKD.

INDEX TERMS Entanglement, photon addition, photon subtraction, hybrid CV-DV entangled states, teleportation, entanglement swapping, entanglement distribution, hybrid quantum communication networks, entanglement-based hybrid QKD.

I. INTRODUCTION

Quantum information processing (QIP) opens new avenues for various applications including high-performance computing, high-precision sensing, and secure communications [1]–[3]. Among various QIP attributes, entanglement is a unique QIP feature: enabling quantum computers capable of solving the problems that are numerically intractable for classical computers, promising quantum-enhanced sensors with measurement sensitivities that exceed the classical limit, and providing certifiable security for data transmission whose security is guaranteed by the laws of quantum mechanics—rather than the unproven assumptions used in cryptography based on computational security.

The associate editor coordinating the review of this manuscript and approving it for publication was Parul Garg.

The distribution of entanglement over long distances has been an outstanding challenge due to photon losses, i.e., quantum signals cannot be amplified without introducing additional noise that degrades or even completely destroys the initial entanglement. Hence, the quantum communication (QuCom) calls for fundamentally distinct loss-mitigation mechanisms to establish long-range entanglement. In this regard, quantum repeaters are being pursued (over the last decade) to overcome the exponentially low entanglement distribution rate versus transmission distance in optical fibers. Despite encouraging advances from the use of silicon vacancy defects in diamond quantum memories to surpass the repeaterless key-generation bound [4], several technological hurdles must be overcome before developing fully functional quantum repeaters for long-distance QuComs, including the scalability of quantum devices, indistinguishability of

emitted photons, and practical quantum error correction (QEC). An alternative solution leveraged satellites as relays for QuCom over thousands of kilometers by virtue of the more favorable quadratic scaling of photon loss versus the distance in free-space optical (FSO) links. Remarkably, quantum key distribution [5], quantum teleportation [6], and entanglement distribution [7] were demonstrated in a ground-to-satellite QuCom testbed across several-thousand kilometers, showing tremendous potential to build up a satellite-mediated wide-area quantum communication network (QCN) via FSO links, in similar fashion as we proposed in [8]. At present, while QuComs are individually validated over specific types of quantum point-to-point links, the QCN that enables full integration of diverse QIP devices into a unified network must still be developed. In particular, the distribution of a large number of quantum states in multiaccess environment over various QCN topologies remains an open problem [9], [10].

To take advantage of quantum resources for QIP [2]–[18], distributed quantum computing, quantum networking, and distributed quantum sensing, it is necessary to interface quantum systems based on different encodings of information (either discrete or continuous). To illustrate, most of the current approaches for quantum computers employ the discrete-variable (DV) encoding of information, while continuous-variable (CV) bosonic, loss-tolerant, quantum systems are known to be more suitable for QCNs and future quantum Internet. Furthermore, hybrid DV-CV QCNs can enable the deterministic teleportation of DV states [11].

Even though entanglement distribution over point-to-point links has been demonstrated, the distribution of a large number of entangled states remains elusive. To this end, efficient and robust interfacing between CV and DV quantum nodes can enable the distribution of quantum states over wavelength-transparent hybrid DV-CV multi-hop, multi-user networks with arbitrary network topology. Thus, developing the means to connect DV and CV optical quantum systems will be a major step-forward to achieve optical quantum interconnects and networks, as we propose in this paper. Figure 1 illustrates the proposed hybrid CV-DV network. The nodes comprising transmitters and receivers capable of generating DV, CV, and hybrid DV-CV entangled states represent the quantum network backbone. Bell-state measurements (BSMs) then perform teleportation and entanglement swapping operations for the CV-to-DV and DV-to-CV information transfer and interconnection between the different type of nodes. Here we propose efficient approaches to hybrid DV-CV entanglement generation, teleportation, and entanglement swapping by employing photon addition [12] and photon subtraction [13] modules.

The goal of this paper is to lay the groundwork for the development of a robust and efficient hybrid CV-DV quantum network, enabling the distribution of a large number of entangled states over hybrid DV-CV multi-hop nodes in an arbitrary topology. The proposed hybrid quantum communication network will serve as the backbone for a future

quantum Internet, thus providing extensive long-term impacts on the economy and national security through QIP, distributed quantum computing, quantum networking, and distributed quantum sensing. The proposed hybrid DV-CV quantum networking concept, employing photon addition modules, will significantly contribute to the endeavors of the future US and global quantum information infrastructure and quantum Internet technologies. The hybrid CV-DV networks have been studied before [14]–[18]. However, previous proposals have not provided a unifying framework to enable future hybrid CV-DV networks by describing how to solve existing problems in a simultaneous manner. Specific contributions can be summarized as follows: 1) we proposed how to generate the hybrid DV-CV entangled states by employing the photon addition modules, 2) we proposed corresponding DV-CV teleportation and entanglement swapping schemes through entangling measurements, 3) we proposed a hybrid DV-CV transparent quantum networking based on photon addition modules including hybrid CV-DV cluster state-based networking concept, 4) we describe how to distribute a large number of entangled states, 5) we describe different approaches to extend the distance between hybrid quantum nodes including reconfigurable quantum LDPC coding, and 6) we described the entanglement based hybrid CV-DV QKD concept.

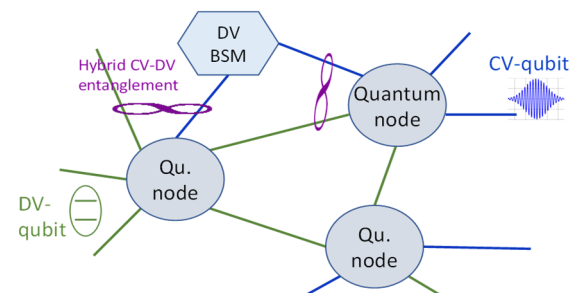


FIGURE 1. Illustration of the proposed hybrid DV-CV quantum communication network. BSM: Bell state measurement. “Qu.”: Quantum.

In the rest of this section the organization of the paper is provided. For completeness of the presentation, the photon addition and photon subtraction modules are introduced in Sec. II. To illustrate the power of the photon addition concept in the same section we describe how to entangle two independent DV states by employing the photon addition modules. In Sec. III we describe our proposal to generate hybrid CV-DV entangled states by employing delocalized photon addition. In Sec. IV we propose how to perform teleportation and entanglement swapping of hybrid states through entangling measurements. In Sections V–VII we describe our proposals on how to extend the transmission distance between nodes in hybrid QCN by employing entangled macroscopic light states (Sec. V), noiseless amplification (Sec. VI), and reconfigurable quantum LDPC coding (Sec. VII). In Sec. VIII we propose how to implement the deterministic cluster state-based networking and distributed computing by utilizing the

photon addition concept. In Sec. IX we describe the proposed entanglement-based hybrid QKD concept. Finally, Sec. X is predicted for concluding remarks.

II. PHOTON ADDITION AND SUBTRACTION MODULES AND ENTANGLING INDEPENDENT DV STATES

To facilitate our description of the proposed hybrid CV-DV networking concepts, first we briefly describe the photon addition and photon subtraction modules. We further describe how the photon addition modules can be used to entangle two independent DV states.

The photon addition module is based on parametric down conversion (PDC), as we illustrate in Figure 2. In Figure 2(a), we illustrate the well-known heralded generation of single-photon states. The photon addition concept is applicable to both CV and DV states. By replacing the vacuum state in the input signal port by a CV state $|\alpha\rangle$ (DV state $|\psi\rangle$), as shown in Fig. 2(b), we are able to add a single photon to the CV (DV) state to get $a^\dagger |\alpha\rangle$ ($a^\dagger |\psi\rangle$) state, where a^\dagger is the creation operator. When the single-photon detector (SPD) is removed in Fig. 2(a), we obtain the common entanglement source, generating the two-mode squeezed vacuum (TMSV) states. The TMSV state has the following representation in the Fock basis:

$$|\psi\rangle_{s,i} = (N_s + 1)^{-1/2} \sum_{n=0}^{\infty} [N_s / (N_s + 1)]^{n/2} |n\rangle_s |n\rangle_i, \quad (1)$$

with the mean photon number being $N_s = \langle \hat{a}_s^\dagger \hat{a}_s \rangle = \langle \hat{a}_i^\dagger \hat{a}_i \rangle$, with corresponding signal and idler annihilation operators denoted by \hat{a}_s and \hat{a}_i , respectively.

The corresponding scheme to entangle two independent DV states, employing the single photon addition concept is provided in Fig. 2(c). With the help of the power splitter, the same pump laser is used for both photon addition modules. The DV states are used at the signal input ports of photon addition modules. We need to use SPDs at idler ports to herald the photon additions. By interacting the idler modes at the beam splitter we are not able anymore to distinguish whether the click on SPD1 (SPD2) originated from the upper or lower branch of single photon addition modules and thus we effectively entangled the signal photons' states. This entangling scheme, except for SPDs, is suitable for integration on the same chip, for instance by using the lithium niobate technology.

A beam splitter can perform a single-photon subtraction, as we illustrate in Figure 3. The operation of a beam splitter (BS) can be described by the following unitary transformation $\hat{U} = \exp[j\theta(\hat{a}^\dagger \hat{b} + \hat{a} \hat{b}^\dagger)]$, where θ is the parameter of the BS, which is related to transmissivity T by $T = \cos^2 \theta$. Clearly, for small θ (high BS transmissivity) the action on input state $|\alpha\rangle |0\rangle$ will be:

$$\begin{aligned} |\psi\rangle_{out} &= \exp[j\theta(\hat{a}^\dagger \hat{b} + \hat{a} \hat{b}^\dagger)] |\alpha\rangle |0\rangle \\ &\cong |\alpha\rangle |0\rangle + j\theta(\hat{a}^\dagger \hat{b} + \hat{a} \hat{b}^\dagger) |\alpha\rangle |0\rangle \\ &= |\alpha\rangle |0\rangle + j\theta(\hat{a} |\alpha\rangle) |1\rangle. \end{aligned} \quad (2)$$

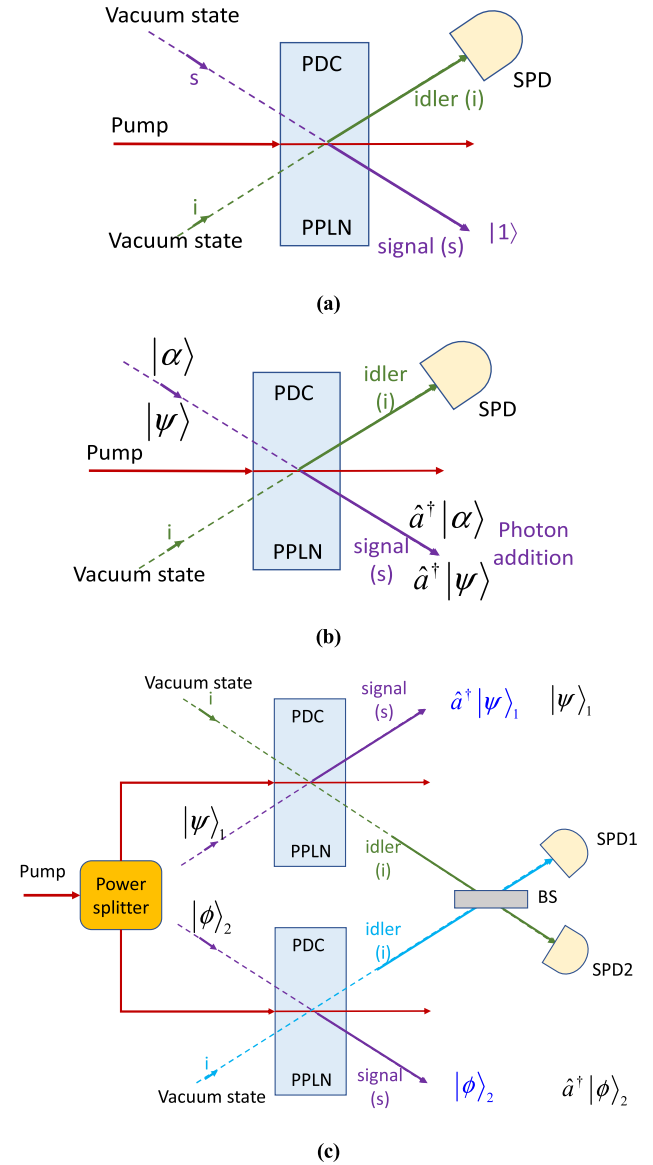


FIGURE 2. The illustration of a single-photon addition: (a) generation of the signal photon states, (b) photon addition module, and (c) entangling two independent DV states. SPD: single-photon detector; PDC: parametric down conversion; PPLN: periodically poled lithium niobate crystal; BS: beam splitter.

Detection of a photon by the SPD heralds the single-photon subtraction at other output port. Photon addition and subtraction will be the two basic entanglement engineering operations to enable generation of hybrid CV-DV entangled states, their teleportation, and entanglement swapping.

III. GENERATION OF HYBRID DV-CV ENTANGLED STATES BY DELOCALIZED PHOTON ADDITION

The photon addition modules can entangle two independent DV quantum states, as we illustrate in Figure 4. When the photon gets detected on SPD1 (SPD2), we will not know if it originated from the upper or the lower photon addition module. This inability to distinguish between two possibilities will

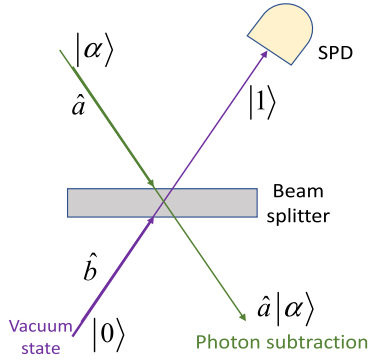


FIGURE 3. The Illustration of a single-photon subtraction concept by a beam splitter.

indicate that the following quantum state

$$|\psi\rangle_{out} = 2^{-1/2} \left[(\hat{a}^\dagger |\psi\rangle) |\phi\rangle + |\psi\rangle (\hat{a}^\dagger |\phi\rangle) \right] \quad (3)$$

is entangled.

When the DV state $|\phi\rangle_2$ in Fig. 4 get replaced by the CV state $|\alpha\rangle_2$, we will be able to generate the hybrid DV-CV state as we illustrate in Figure 5. Similarly to Fig. 4, when the photon gets detected on SPD1 (SPD2) we will not know if it originated from the upper or lower photon addition module. This inability to distinguish between two cases will indicate that the following hybrid DV-CV state

$$|\psi\rangle_{out} = 2^{-1/2} \left[(\hat{a}^\dagger |\psi\rangle) |\alpha\rangle + |\psi\rangle (\hat{a}^\dagger |\alpha\rangle) \right] \quad (4)$$

is entangled.

The photon addition can also apply to the *multipartite entangled states*. Let us assume that the two input states to the quantum circuit in Figure 4 are multipartite with M and N qubits, respectively. By performing the delocalized photon addition on the M^{th} qubit from the top multipartite state and on the first qubit on the bottom multipartite state, once the photons are detected on SPDs, we effectively heralded the multipartite state with $(M + N)$ qubits.

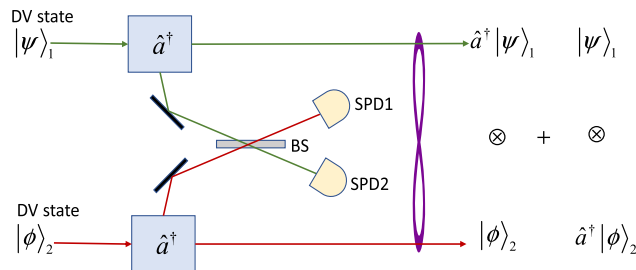


FIGURE 4. Scheme to entangle two independent DV quantum states by delocalized photon addition with one possible implementation provided in Fig. 2(c).

IV. HYBRID CV-DV STATES TELEPORTATION AND ENTANGLEMENT SWAPPING THROUGH ENTANGLING MEASUREMENTS

To perform entanglement swapping between DV only and hybrid DV-CV nodes, we can use the two-photon subtraction approach shown in Fig. 6. When the SPD1 (SPD2) clicks,

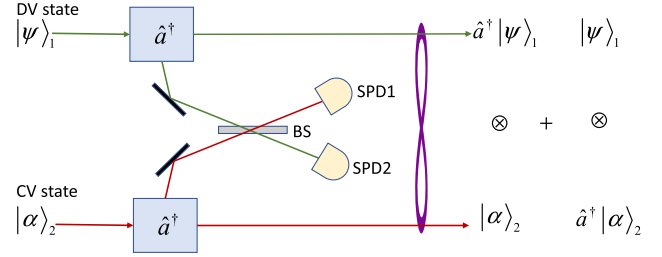


FIGURE 5. Generating an entangled hybrid DV-CV state by delocalized photon addition.

we do not know whether the signal originates from photon subtracted from a DV state $|\phi\rangle_2$ or a DV state $|\psi\rangle_3$, and this uncertainty entangles DV state $|\psi\rangle_1$ and CV state $|\alpha\rangle_4$, effectively performing entanglement swapping.

The entanglement swapping and teleportation can be implemented as we illustrate in Fig. 7, in which an intermediate node distributes the entanglement. In this scenario, Bob possesses a CV state, while Alice a hybrid DV-CV state. Alice mixes her CV mode (from the hybrid state) with the TMSV mode on beam splitter. To characterize this input, we can use the characteristic function, defined as $\chi_{in}(\alpha) = \langle D(\alpha) \rangle$, where $D(\alpha)$ is the displacement operator. $\chi_{TMSV}(\alpha^*, \alpha) = \exp[-|\alpha|^2 \exp(-2r)]$ can determine the TMSV state characteristic function, where r is the squeezing parameter. Alice performs the homodyne detection on beam splitter outputs to obtain μ and transmits it over a classical channel to Bob, who uses it to perform the displacement operator $D(\mu)$ on his qubit from the TMSV pair. Bob's characteristic function is given by $\chi_{out}(\alpha) = \chi_{in}(\alpha) \chi_{TMSV}(\alpha^*, \alpha)$. Clearly, only when $r \rightarrow \infty$ will Bob be able to perfectly recover Alice's transmitted state, since then $\chi_{TMSV}(\alpha^*, \alpha) \rightarrow 1$.

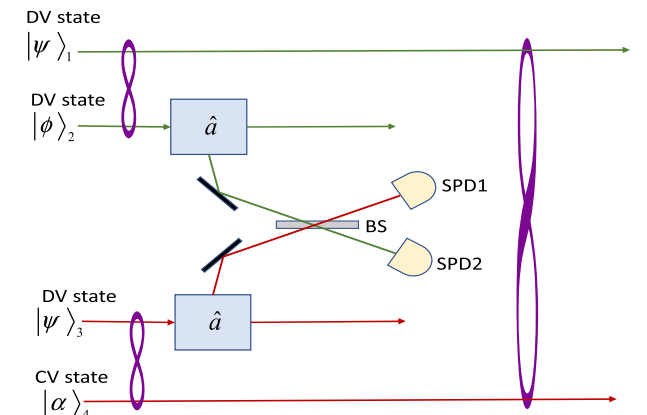


FIGURE 6. Entanglement swapping between DV only node and hybrid DV-CV node by two-photon subtraction.

Very often the Schrödinger's cat states are used to represent the CV qubits [14], [18] as follows: $|\psi_{CV}\rangle = N_{\pm}(|\alpha\rangle \pm |-\alpha\rangle)$, where N_{\pm} is the normalization factor. The cat states are typically obtained as the approximation of single-mode squeezed vacuum states for properly chosen squeezing parameter r , such as $r = 0.18$ [14]. Unfortunately, such generated cat

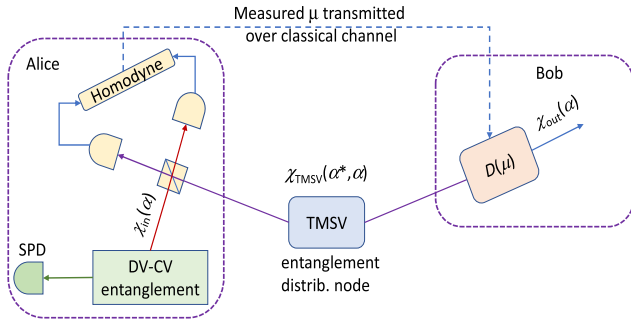


FIGURE 7. Entanglement swapping and teleportation in which an intermediate node distributes the entanglement.

states are not very tolerant to loss. On the other hand, the entangled-photon holes introduced by Franson [26] exhibit good tolerance to loss and amplification [27] that can be generated as shown in Fig. 8.

Two-photon subtraction can be represented by $|\psi\rangle = \hat{a}\hat{b}S_2(z)|0,0\rangle$, where $S_2(z)$ is the two-mode squeezing operator $S_2(z) = e^{z\hat{a}^\dagger\hat{b}^\dagger - z^*\hat{a}\hat{b}}$, with $z = r\exp(j\theta)$. If we introduce a new basis $\hat{a}_+ = 2^{-1/2}(\hat{a} + \hat{b})$, $\hat{a}_- = 2^{-1/2}(\hat{a} - \hat{b})$, we can write $S_2(z)$ as product of two single-mode squeezing operators $S_\pm(\pm z)$. Now, a two-photon subtracted state can be represented in a form similar to the cat state

$$|\psi\rangle = (\hat{a}_+^2 S_+ |0\rangle)(S_- |0\rangle) - (S_+ |0\rangle)(\hat{a}_-^2 S_- |0\rangle), \quad (5)$$

but does not require the squeezing parameter to be low.

In incoming three sections we describe our proposed approaches to extend the distance between neighboring nodes in the hybrid CV-DV quantum network.

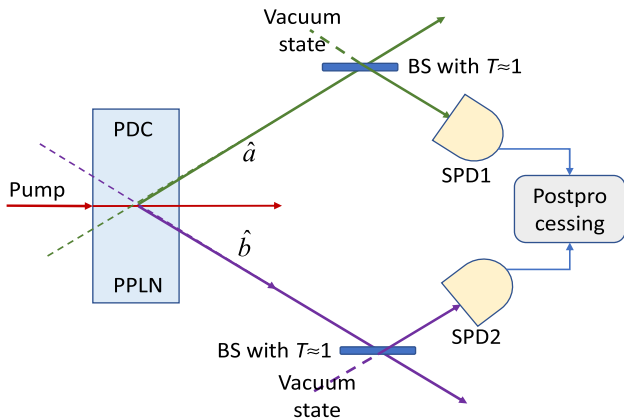


FIGURE 8. Generating entangled-photon holes-embedded TMSV states.

V. EXTENDING THE TRANSMISSION DISTANCE BETWEEN QUANTUM NODES BY EMPLOYING THE ENTANGLED MACROSCOPIC LIGHT STATES

To extend the transmission distance between the quantum nodes, we can use the macroscopic light states as CV states, based on recent finding that macroscopic light states can

be entangled [28]. The corresponding scheme to generate entangled CV-CV macroscopic states is shown in Fig. 9. The output state can be represented by

$$|\psi\rangle = \mathfrak{N}^{-1/2}(\hat{a}^\dagger |\alpha\rangle_1 |\beta\rangle_2 + e^{i\phi} |\alpha\rangle_1 \hat{b}^\dagger |\beta\rangle_2), \quad (6)$$

where \mathfrak{N} is the normalization factor. The phase shift needs to be properly chosen to ensure that the output macroscopic states are entangled. By using the following property of the displacement operator $\hat{a}^\dagger D(\alpha) = D(\alpha)(\hat{a}^\dagger + \alpha^*)$, we can rewrite the output states as follows:

$$|\psi\rangle = \mathfrak{N}^{-1/2} D_1(\alpha) D_2(\beta) \left(|1\rangle |0\rangle + e^{i\phi} |0\rangle |1\rangle \right) + \mathfrak{N}^{-1/2} \alpha^* \left(1 + e^{i\phi} \right) |\alpha\rangle |\beta\rangle. \quad (7)$$

Clearly, the first state is an entangled state, while the second state is a separable state. Now, by setting $\phi = \pi$, the second term becomes zero and the scheme shown in Fig. 9 can indeed entangle the macroscopic CV states that are tolerant to losses. This approach allows the distances between nodes to significantly increase.

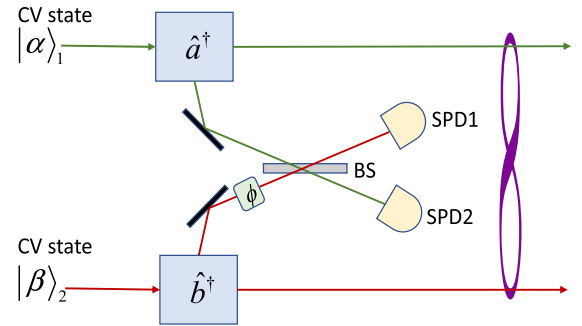


FIGURE 9. Generating macroscopic entangled CV-CV states.

VI. EXTENDING THE TRANSMISSION DISTANCE BETWEEN QUANTUM NODES BY NOISELESS AMPLIFICATION

To extend the transmission distance between quantum nodes in hybrid CV-DV networks the noiseless amplification can be potentially used. The amplification process can typically be represented by:

$$a \rightarrow b = \sqrt{G}a + n; \langle n \rangle = 0, \quad \langle n^\dagger n \rangle \neq 0 \quad (8)$$

where b is the amplifier output mode, G is the amplifier gain, while n is the noise mode. Clearly, the signal-to-noise ratio (SNR) get deteriorated since:

$$\langle b^\dagger b \rangle = G a^\dagger a + \sqrt{G} (a^\dagger n + n^\dagger a) + n^\dagger n, \quad (9)$$

indicating the amplified mode get affected by signal-noise and noise terms.

To solve for this problem, Bellini's group [29], [30] proposed the heralded photon amplifier in which the photon addition is followed by the photon subtraction so that

the input state, represented by the density operator ρ , get mapped to:

$$\rho \rightarrow a(a^\dagger \rho a) a^\dagger. \quad (10)$$

When the input of the noiseless amplifier is in superposition state $\rho = \alpha|0\rangle\langle 0| + \beta|1\rangle\langle 1|$, the input state is mapped to:

$$\rho \rightarrow 2\beta|1\rangle\langle 1|, \quad (11)$$

indicating that the single photon state acquires the gain of 2 and the noise is not added.

VII. EXTENDING THE TRANSMISSION DISTANCE BETWEEN QUANTUM NODES BY RECONFIGURABLE QUANTUM LDPC (QLDPC) CODING

To extend the transmission distance between nodes, we also propose to use the *QEC-based quantum networking that employs QLDPC coding* [20], wherein the corresponding QLDPC code comprises multiple subcodes. Figure 10 illustrates the proposed concept. An information state of K qubits is encoded by a systematic $[N, K]$ QLDPC code to obtain the codeword $|q_t\rangle$. Intermediate quantum-node simple syndrome decoding identifies the most probable quantum-error operator and corrects it. After that, the re-encoding takes place by inserting additional redundant qubits. Therefore, we progressively improve the error correction strength based on the number of intermediate nodes. The QLDPC soft-decision decoding takes place at the destination node.

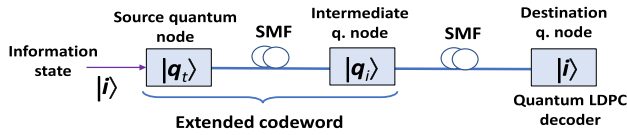


FIGURE 10. Extending the distance between two nodes in a QCN by a reconfigurable QLDPC code, wherein in each intermediate node extra redundant qubits are added. In each intermediate node, simple syndrome decoding identifies the most probable error operator and corrects it before the re-encoding takes place. The QLDPC soft-decision decoding takes place at the destination node.

VIII. HYBRID DV-CV QUANTUM NETWORKING BASED ON DETERMINISTIC CLUSTER STATE CONCEPT

The cluster state-based quantum networking concept was introduced in our previous paper [8]. When the cluster C is defined as a connected subset on a d -dimensional lattice, it obeys the set of eigenvalue equations $S_a|\phi\rangle_C = |\phi\rangle_C$, where $S_a = X_a \otimes_{b \in N(a)} Z_b$ are *stabilizer operators* with $N(a)$ denoting the neighborhood of $a \in C$. To create a 2-D cluster state, the approach proposed by Gilbert *et al.* [23] was employed in [8]. This utilizes linear states (generated by spontaneous PDC, local unitaries, and type I fusion) to create the desired 2-D cluster state. The type I fusion [23] is composed of the polarization beam splitter (PBS), 45° polarization rotator, and the SPD. The PBS reflects the vertical photon, while the horizontal photon gets transmitted through the PBS. Given the probabilistic nature of the PBS, when photons are present at both input ports, there exist four possible

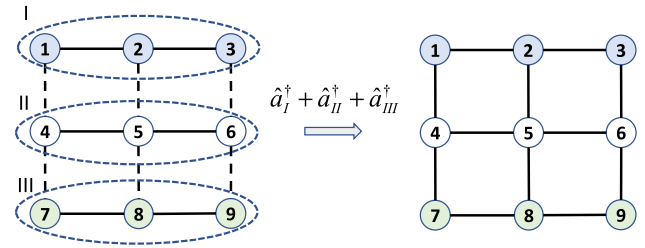


FIGURE 11. Creation of 9-node 2-D cluster state from three linear cluster states by using the delocalized photon addition.

outcomes each occurring with a probability of 0.25. Two outcomes correspond to the desired fusion operators, and the success probability of the fusion is 0.5. When a single photon is detected by the detector, the successful fusion is declared. When the fusion process is not successful we need to repeat the procedure. Therefore, building the quantum network by employing the fusion process could be both time and resources consuming.

To solve for this problem, we propose to employ the *photon addition concept* introduced in Figs. 4-5, wherein the quantum states to be entangled are now the cluster states. The key advantage versus the type I fusion is that the creation of a desired cluster state, with the photon addition concept, becomes the deterministic process. Another advantage of the proposed concept is that the qubits in the cluster do not have to be DV or CV only. Namely, the proposed photon addition concept to create the desired cluster state can be applied to all possible types of qubits, including DV, CV, and hybrid DV-CV. Once we create a 2-D cluster state of DV nodes, wherein the qubits locate at different nodes in the QCN, we need to perform measurements on properly selected set of nodes to establish the EPR pairs between arbitrary two nodes in the QCN. From ref. [2] we know that the 2-D DV cluster state is universal. Therefore, we can use the same 2-D network architecture for both the QCN and distributed quantum computing. As an illustration, Fig. 11 illustrate how to create a 2-D cluster state with 9 nodes, starting from three linear cluster states. The dashed lines indicate that the physical links are installed but corresponding nodes are not entangled. By performing the delocalized photon addition between nodes 3-6 and 6-9 we entangle three linear cluster states and effectively create the 2-D 9-node cluster state. This cluster state is suitable for distributed quantum computing. To establish EPR pairs between any two nodes we need to perform properly selected Y and Z measurements as described in ref. [8]. If we are not interested in distributed quantum computing or sensing but just in quantum networking the cluster state concept is not really needed because we can create arbitrary quantum network topology by performing the delocalized photon additions on properly chosen nodes in the network. Such a hybrid quantum network allows the distribution of large number of entangled states at long-distance by using the photon addition concept.

IX. ENTANGLEMENT-BASED (EB) HYBRID CV-DV QKD NETWORKS

The hybrid CV-DV QKD has already been discussed in our previous paper [31], in which both DV and CV degrees of freedom are encoded on the same coherent state. With the help of an optical switch Bob randomly selects DV or CV receiver and shares this information with Alice. Alice and Bob then perform sifting procedure on both CV and DV subsystems. The information reconciliation is further applied on CV and DV raw keys so that the corrected key corresponding to hybrid scheme is obtained, followed by privacy amplification to obtain the secure key. An interested reader is referred to ref. [31] for additional details on coherent state-based hybrid QKD. The hybrid QKD scheme proposed here is based on entangled hybrid states obtained by localized photon addition concept introduced in Figs. 4 and 5. In this protocol, Alice simultaneously encodes her CV and DV qubits and Bob simultaneously measures his CV and DV qubits by randomly selected DV basis and CV basis. This protocol represents a generalization of both CV and DV protocols. Given that this entanglement-based (EB) hybrid QKD scheme does not require the use of the optical switch higher secret-key rates (SKRs) can be obtained compared to coherent state-based hybrid QKD scheme [31]. There are different options how such entangled states, suitable for hybrid QKD, can be obtained. For instance, we can create first separate entangled DV-DV and CV-CV states and entangle them further by another photon addition stage, which is illustrated in Fig. 12. The same pump laser can be used for all photon addition modules, with the help of the power splitter.

In another scenario, Alice can start with two independent coherent state $|\alpha\rangle_A$ and DV state $|\phi\rangle_A$ and encode them separately and use them at the input of photon addition module (to entangle them). At the same time she can prepare two independent coherent state $|\beta\rangle_B$ and DV state $|\psi\rangle_B$ for Bob and entangle them in another photon addition module. In the second photon addition stage she will further entangle her and Bob's hybrid states. On receiver side, Bob will perform simultaneous measurements on his CV and DV qubits and recover Alice transmitted sequences provided that he used the same DV basis and CV basis. Therefore, this version of EB hybrid QKD protocol is generalization of the protocol introduced in [31], and the corresponding SKR expression is similar to Eq. (1) in ref. [31].

As an illustration, let us assume the DV state employs the decoy state protocol while CV state the optimized 8-state protocol [32]. Alice independently encodes these two states and further entangles them with the help of the photon addition modules, according to Fig. 12. Bob simultaneously randomly selects the DV basis and the CV basis and performs measurements on his CV and DV states, according to Fig. 12, at the same time. After basis reconciliation, the obtained DV and CV sequences are interleaved and encoded by a systematic LDPC code. In reverse reconciliation, Bob sends the parity bits for interleaved CV-DV sequence over an authenticated public channel to Alice. Alice performs LDPC decoding on

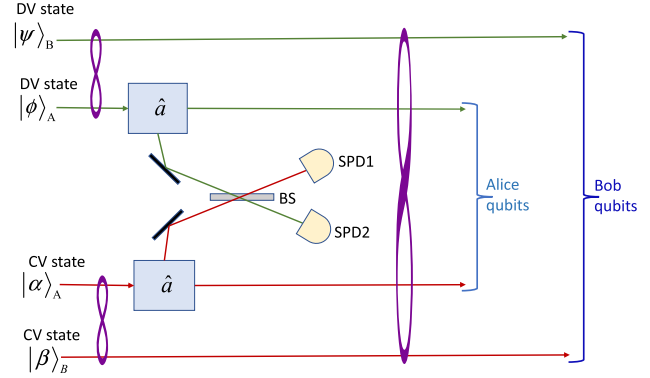


FIGURE 12. Illustrating the generation of hybrid state suitable for use in entanglement-based hybrid QKD.

her sequence, with the side information in the form of parity bits received from Bob. After that the conventional privacy amplification over decoded interleaved (corrected) sequence takes place. Even though that the DV sequence can be significantly shorter compared to the CV sequence, given that security of discrete CV modulation schemes is known only for linear channels, the employment of DV subsystem can guaranty the security of both subsystems for arbitrary quantum channels. The resulting SKR will be equal to the sum of SKRs of individual DV and CV subsystems, wherein the parameters on both subsystems are simultaneously optimized to maximize the overall SKR.

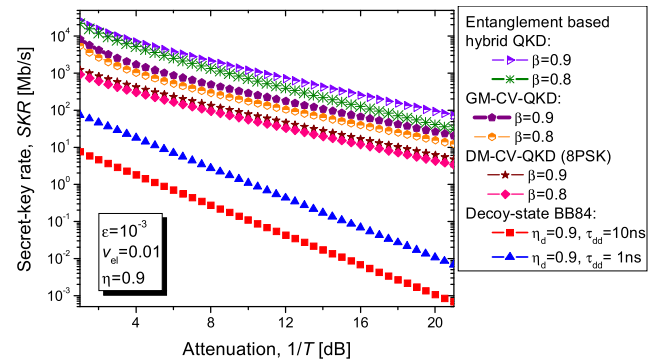


FIGURE 13. SKRs vs. channel loss of entanglement-based hybrid CV-DV QKD against GM-CV-QKD, DM-CV-QKD (8PSK), and decoy state BB84 protocols. Raw signaling rate of CV-QKD subsystem was set to 10 Gb/s.

To illustrate the advantages of the proposed EB hybrid scheme against the conventional decoy-state BB84, Gaussian modulation (GM) based CV-QKD, and discrete modulation (DM) based CV-QKD with 8PSK protocols, we apply decoy-state BB84 with time-phase encoding protocol on DV state and DM-CV-QKD protocol on CV state before entangling them as described above. The DM-CV-QKD protocol is based on 8-star-QAM introduced in ref. [32]. The SKR results are summarized in Fig. 13. The CV-QKD subsystem parameters are selected as follows: the excess noise variance is $\epsilon = 10^{-3}$, electrical noise variance is set to $v_{en} = 0.01$, and detector efficiency is $\eta = 0.9$. The ratio of outer circle

(containing four points) and inner circle (containing other four points) radii in 8-star-QAM is 1.35. On the other hand, the decoy-state BB84 subsystem parameters are selected as: dark current rate $p_d = 10^{-6}$, the detection efficiency $\eta_d = 0.9$, the dead time of SPDs is $\tau_{dd} = 10$ ns, the error correction (in)efficiency is $f_e = 1.1$, and the intrinsic misalignment error rate is 0.005. From Fig. 13 we can conclude that the EB hybrid QKD scheme, described above, outperforms both GM-CV-QKD and DM-CV-QKD (with 8PSK) QKD schemes for all channel losses and both reconciliation efficiencies $\beta = 0.9$ and $\beta = 0.8$ (under study). The EB hybrid QKD scheme significantly outperforms the decoy-state BB84 protocol.

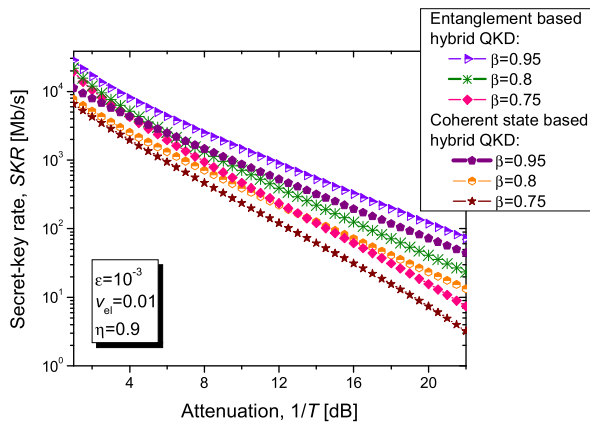


FIGURE 14. SKRs vs. channel loss of proposed entanglement-based hybrid CV-DV QKD against coherent state-based hybrid QKD with insertion loss of optical switch being 2 dB. Raw signaling rate of CV-QKD subsystem was set to 10 Gb/s.

On the other hand, in Fig. 14 we compare the EB hybrid QKD against corresponding coherent state-based hybrid QKD scheme [31] for MEMS-based optical switch of insertion loss of 2 dB. Clearly, the SKRs for EB hybrid QKD scheme are higher than SKRs for coherent state-based hybrid QKD scheme for all three reconciliation efficiencies considered $\beta = 0.95, 0.8$, and 0.75 . As the channel loss increases the gap between corresponding curves is getting more pronounced. Therefore, the EB hybrid QKD scheme represents a promising candidate to increase the SKR. Moreover, by employing the photon addition concept the EB hybrid QKD scheme can be extended to the multipartite DV and CV states and overall SKRs can be further improved. Alternatively, for fixed SKR, the transmission distance between neighboring nodes in the QKD network can be extended.

X. CONCLUDING REMARKS

Purpose of this paper has been to lay the groundwork for the development of a robust and efficient hybrid CV-DV quantum network enabling the distribution of a large number of entangled states over hybrid DV-CV multi-hop nodes in an arbitrary topology. The proposed hybrid CV-DV QCN can serve as the backbone for the future quantum Internet.

By employing the photon addition and photon subtraction modules we have described how to generate entangled CV-DV states. We have also described how to implement teleportation and entanglement swapping of hybrid states by using the entangling measurements. To extend the transmission distance between nodes in hybrid QCN we have proposed the employment of entangled microscopic states, noiseless amplification, and reconfigurable QLDPC coding. To perform simultaneously quantum networking and distributed quantum computing we proposed the usage of deterministic cluster state concept enabled by the photon addition modules. Finally, we have proposed the EB hybrid QKD concepts outperforming the existing QKD schemes suitable for use in future hybrid QKD networks.

REFERENCES

- [1] G. Cariolaro, *Quantum Communications*. Cham, Switzerland: Springer, 2015.
- [2] I. B. Djordjevic, *Quantum Information Processing, Quantum Computing, and Quantum Error Correction: An Engineering Approach*. London, U.K.: Elsevier, 2021.
- [3] I. B. Djordjevic, *Physical-Layer Security and Quantum Key Distribution*. Cham, Switzerland: Springer, 2019.
- [4] M. Bhaskar, R. Riedinger, B. Machielse, and D. Levonian, "Experimental demonstration of memory-enhanced quantum communication," *Nature*, vol. 580, p. 60, Oct. 2020.
- [5] S. Liao, W. Cai, W. Liu, L. Zhang, Y. Li, J. Ren, and J. Yin, "Satellite-to-ground quantum key distribution," *Nature*, vol. 549, p. 43, Aug. 2017.
- [6] J. Ren, P. Xu, H. Yong, L. Zhang, S. Liao, and J. Yin, "Ground-to-satellite quantum teleportation," *Nature*, vol. 549, p. 70, Oct. 2017.
- [7] J. Yin, Y. Cao, Y. Li, S. Liao, L. Zhang, J. Ren, and W. Cai, "Satellite-based entanglement distribution over 1200 kilometers," *Science*, vol. 356, no. 6343, pp. 1140–1144, Jun. 2017.
- [8] I. B. Djordjevic, "On global quantum communication networking," *Entropy*, vol. 22, no. 8, p. 831, Jul. 2020.
- [9] *Entanglement Management and Control in Transparent Optical Quantum Networks*, Funding Opportunity Announcement, Dept. Energy, 2015.
- [10] *From Long-Distance Entanglement to Building a Nationwide Quantum Internet*, Report of the DOE Quantum Internet Blueprint Workshop, Dept. Energy, SUNY Global Center, New York, NY, USA, Feb. 2020.
- [11] S. Takeda, T. Mizuta, M. Fuwa, P. van Loock, and A. Furusawa, "Deterministic quantum teleportation of photonic quantum bits by a hybrid technique," *Nature*, vol. 500, p. 315, Dec. 2013.
- [12] A. Zavatta, S. Viciani, and M. Bellini, "Quantum-to-classical transition with single-photon-added coherent states of light," *Science*, vol. 306, p. 660, Oct. 2004.
- [13] A. Zavatta, V. Parigi, M. S. Kim, and M. Bellini, "Subtracting photons from arbitrary light fields: Experimental test of coherent state invariance by single-photon annihilation," *New J. Phys.*, vol. 10, no. 12, Dec. 2008, Art. no. 123006.
- [14] A. E. Ulanov, D. Sychev, A. A. Pushkina, I. A. Fedorov, and A. I. Lvovsky, "Quantum teleportation between discrete and continuous encodings of an optical qubit," *Phys. Rev. Lett.*, vol. 118, Jan. 2017, Art. no. 160501.
- [15] S.-W. Lee and H. Jeong, "Near-deterministic quantum teleportation and resource-efficient quantum computation using linear optics and hybrid qubits," *Phys. Rev. A, Gen. Phys.*, vol. 87, no. 2, Feb. 2013, Art. no. 022326.
- [16] S. Takeda, M. Fuwa, P. van Loock, and A. Furusawa, "Entanglement swapping between discrete and continuous variables," *Phys. Rev. Lett.*, vol. 114, Mar. 2015, Art. no. 100501.
- [17] K. Huang, H. L. Jeannic, O. Morin, T. Darras, G. Guccione, A. Cavaillès, and J. Laurat, "Engineering optical hybrid entanglement between discrete and continuous-variable states," *New J. Phys.*, vol. 21, no. 8, Aug. 2019, Art. no. 083033.
- [18] G. Guccione, T. Darras, H. Le Jeannic, and V. Verma, "Connecting heterogeneous quantum networks by hybrid entanglement swapping," *Sci. Adv.*, vol. 6, no. 22, May 2020, Art. no. eaba4508.

- [19] DOE Workshop Quantum Networks for Open Science report. Accessed: Feb. 24, 2022. [Online]. Available: <https://info.ornl.gov/sites/publications/Files/Pub124247.pdf>
- [20] I. B. Djordjevic, "Quantum LDPC codes from balanced incomplete block designs," *IEEE Commun. Lett.*, vol. 12, no. 5, pp. 389–391, May 2008.
- [21] K. Noh, S. M. Girvin, and L. Jiang, "Encoding an oscillator into many oscillators," *Phys. Rev. Lett.*, vol. 125, Feb. 2020, Art. no. 080503.
- [22] M. Eaton, R. Nehra, and O. Pfister, "Non-Gaussian and Gottesman–Kitaev–Preskill state preparation by photon catalysis," *New J. Phys.*, vol. 21, no. 11, Nov. 2019, Art. no. 113034.
- [23] G. Gilbert, M. Hamrick, and Y. Weinstein, "Efficient construction of photonic quantum-computational clusters," *Phys. Rev. A, Gen. Phys.*, vol. 73, Jun. 2006, Art. no. 064303.
- [24] S. Yokoyama, R. Ukai, S. C. Armstrong, C. Sornphiphatphong, T. Kaji, S. Suzuki, J. Yoshikawa, H. Yonezawa, N. C. Menicucci, and A. Furusawa, "Ultra-large-scale continuous-variable cluster states multiplexed in the time domain," *Nature Photon.*, vol. 7, pp. 982–986, Nov. 2013.
- [25] T. Kim, M. Fiorentino, and F. N. C. Wong, "Phase-stable source of polarization-entangled photons using a polarization Sagnac interferometer," *Phys. Rev. A, Gen. Phys.*, vol. 73, Oct. 2006, Art. no. 012316.
- [26] J. D. Franson, "Entangled photon holes," *Phys. Rev. Lett.*, vol. 96, no. 9, Mar. 2006, Art. no. 090402.
- [27] J. D. Franson, "Quantum communication using entangled photon holes," in *Proc. Frontiers Opt. Sci.*, Rochester, NY, USA, Oct. 2012, Paper FTh2C.1.
- [28] N. Biagi, L. S. Constanzo, M. Bellini, and A. Zavatta, "Entangling macroscopic light states by delocalized photon addition," *Phys. Rev. Lett.*, vol. 124, no. 3, Jan. 2020, Art. no. 033604.
- [29] A. Zavatta, J. Fiurák, and M. Bellini, "A high-fidelity noiseless amplifier for quantum light states," *Nature Photon.*, vol. 5, no. 1, pp. 52–56, Jan. 2011.
- [30] C. N. Gagatsos, J. Fiurák, A. Zavatta, M. Bellini, and N. J. Cerf, "Heralded noiseless amplification and attenuation of non-Gaussian states of light," *Phys. Rev. A, Gen. Phys.*, vol. 89, no. 6, Jun. 2014, Art. no. 062311.
- [31] I. B. Djordjevic, "Hybrid QKD protocol outperforming both DV and CV-QKD protocols," *IEEE Photon. J.*, vol. 12, no. 1, pp. 1–8, Feb. 2020.
- [32] I. B. Djordjevic, "Optimized-Eight-State CV-QKD protocol outperforming Gaussian modulation based protocols," *IEEE Photon. J.*, vol. 11, no. 4, Aug. 2019, Art. no. 4500610.



IVAN B. DJORDJEVIC (Fellow, IEEE) received the Ph.D. degree from the University of Niš, Yugoslavia, in 1999.

He is currently a Professor of electrical and computer engineering and optical sciences with The University of Arizona, the Director of the Optical Communications Systems Laboratory (OCSL) and the Quantum Communications (QuCom) Laboratory, and the Co-Director of the Signal Processing and Coding Laboratory.

Prior to joining The University of Arizona, he held appointments at the University of Bristol, U.K.; the University of the West of England, U.K.; Tyco Telecommunications, USA; the National Technical University of Athens, Greece; and State Telecommunication Company, Yugoslavia. He has authored or coauthored ten books, more than 550 journals and conference publications, and holds 54 U.S. patents.

Dr. Djordjevic is a fellow of OSA (Optica). He serves as an Area Editor/an Associate Editor/a Member of Editorial Board for the following journals: IEEE TRANSACTIONS ON COMMUNICATIONS, IEEE/OSA JOURNAL OF OPTICAL COMMUNICATIONS AND NETWORKING, *Optical and Quantum Electronics*, and *Frequenz*. He was serving as an Editor/a Senior Editor/an Area Editor for IEEE COMMUNICATIONS LETTERS, from 2012 to 2021. He was serving as an Editorial Board Member/an Associate Editor for *Journal of Optics* (IOP) and *Physical Communication* (Elsevier), from 2016 to 2021.

• • •